Nuclear Inst. and Methods in Physics Research, A 1006 (2021) 165328

Contents lists available at ScienceDirect

Nuclear Inst. and Methods in Physics Research, A

journal homepage: www.elsevier.com/locate/nima

A continuous-wave superconducting linear accelerator scheme for the drive beam acceleration of the Compact Linear Collider

Jiayang Liu [a,b,c], Alexej Grudiev [c], Hao Zha [a,b,c,*], Jiaru Shi [a,b], Huaibi Chen [a,b]

[a] Department of Engineering Physics, Tsinghua University, Beijing CN-100084, China
[b] Key Laboratory of Particle and Radiation Imaging (Tsinghua University), Ministry of Education, Beijing CN-100084, China
[c] European Organization for Nuclear Research, CERN CH-1211, Geneva 23, Switzerland

ARTICLE INFO

Keywords:
Compact Linear Collider
Superconducting linear accelerator
Drive beam
Beam-loading compensation

ABSTRACT

The Compact Linear Collider (CLIC) utilizes two 2.5-km-long normal-conducting linear accelerators (LINACs) to produce a drive beam with 140 μs pulse length at a repetition rate of 50 Hz. This setup is relatively expensive in the early stages due to both the length of the drive beam LINACs and the amount of the power sources for one drive beam complex are the same in all energy stages. A new concept of accelerating the CLIC drive beam in superconducting LINACs as an alternative scheme is investigates in this work. This scheme requires a minimal number of power sources at the early stages of the CLIC and consequently has the potential to reduce the entry cost. A dimensionless parameter named capacity factor η which determines the number of the superconducting structures and the power is introduced. Two proof-of-concept schemes to compensate the beam-loading effect are also proposed in this paper. The mixed-structure scheme finally selected as the nominal design achieves an optimum η of approximately 1.16 compared to a value of 50.5 without the beam-loading compensation. A rough estimation on the cost of this scheme has also been studied.

1. Introduction

The Compact Linear Collider (CLIC) is one of the candidate projects of future linear colliders [1,2]. The CLIC utilizes a large-current and low-energy drive beam (DB) to generate X-band radio-frequency (RF) power. The RF power feeds the X-band high-gradient accelerating structures to accelerate the energy of electrons and positrons to 1.5 TeV, which is called as two-beam acceleration (TBA) [3–17]. This TBA scheme converts the power from a long-pulse and low-energy beam to support the short-pulse acceleration. Compared with conventional schemes that use commercial RF power sources, TBA scheme can potentially attain both high gradient and reduced cost for a linear collider in the TeV energy range.

In the current conceptual design report (CDR) of the CLIC with a colliding beam energy of 3 TeV in the center of mass, two normal-conducting (NC) linear accelerators (LINACs) operated in pulse mode with a repetition rate of 50 Hz are used to accelerate the drive beam for the TBA scheme, as shown in Fig. 1. The NC structures operate efficiently in the so-called full beam-loading regime such that the drive beam takes more than 80% of the total peak input power fed from the klystrons as 10 GW per LINAC in the 140 μs pulse length. The drive beam is then delivered into the combiner ring, and all bunches are grouped into 24 sub-trains with a peak current in train of 100 A. Each sub-train is dispatched into one decelerating unit for the X-band RF power generation. This TBA concept has been demonstrated in the CLIC Test Facility (CTF3) [18].

The CLIC is designed to be constructed in three energy stages, namely, 380 GeV, 1.5 TeV, and 3 TeV [19]. The drive beam has a shorter pulse length in the earlier stage. The beam power, however, is determined by the power consumption per length of the main LINAC accelerating structures, which is about the same as 10 GW per LINAC in all energy stages. Therefore, all energy stages require the same quantity of RF power sources and accelerating structures for one drive beam complex working in the pulse mode, which are extremely expensive in the early stages.

In this work, an alternative scheme that utilizes superconducting (SC) LINACs for the drive beam acceleration in the 3 TeV stage of the CLIC is investigated. In this scheme, the cavities and power sources are operated in the continuous-wave (CW) mode, whereas the drive beam is still delivered in the pulse mode. The superconducting radio-frequency (SRF) cavities continuously store electromagnetic power and release the stored energy when the beam comes, as illustrated in Fig. 2. The required input power and structure length for one drive beam complex working in the CW mode is approximately proportional to the total energy gain of the bunches in one beam pulse rather than the beam power. The total energy gain of the bunches in the initial 380 GeV stage of the CLIC is 1/8 of that in the final 3 TeV stage due to the less

* Corresponding author at: Department of Engineering Physics, Tsinghua University, Beijing CN-100084, China.
E-mail address: zha_hao@mail.tsinghua.edu.cn (H. Zha).

https://doi.org/10.1016/j.nima.2021.165328
Received 14 December 2020; Received in revised form 16 March 2021; Accepted 5 April 2021
Available online 8 April 2021
0168-9002/

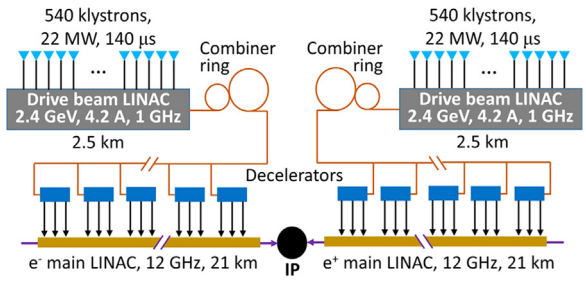

Fig. 1. Layout of two-beam acceleration of for CLIC.

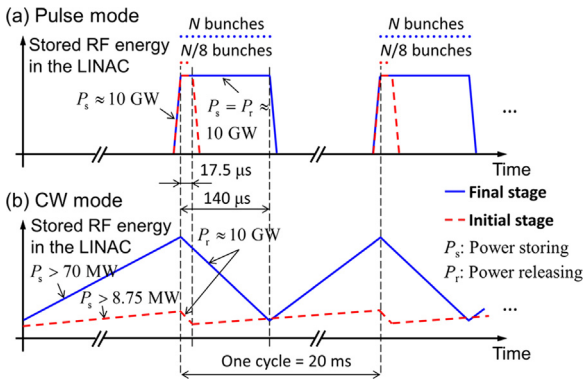

Fig. 2. (a) The pulse mode scheme and (b) CW mode scheme for the CLIC DB LINACs.

bunches of the drive beam. Therefore, the quantity of the power sources and cavities in the initial stage is also 1/8 of that in the final stage with the use of this energy-storing and energy-releasing scheme. In the later stages, more structure units are added but the field amplitude of cavities remains the same as that of earlier stages.

This scheme based on the acceleration of the drive beam by SC technology for the CLIC was firstly proposed by Schnell in 1986 as the original scheme operated in single-bunch mode [15]. An evolution from the single-bunch mode into the multi-bunch operation for the SC DB LINACs was addressed by Thorndahl [16]. The critical problem in that scheme is that the number of the drive beam bunches in one pulse is limited by the strong beam-loading effect, which will cause the decrease of the accelerating voltage during the energy-releasing period. This beam-loading effect will be discussed in Section 3. This problem results in a huge energy variation to the drive beam and may not fit the 1% energy acceptance of the combining and transporting systems [20,21]. Different solutions have been developed to compensate the beam-loading effect, which are described in Sect. 4. Taking the PIP-II HB-650 cavities [22,23], high-power superconducting proton LINAC (HP-SPL) [24], and Large Hardon Collider (LHC) [25,26] as the references, a rough cost estimation on the CLIC SC-DB LINACs is given in Section 5.

The study on two-beam accelerations is also applied on dielectric accelerating structures [6–9] and beam-driven plasma wakefield acceleration [4,5]. Similar applications that use SC structures operated in CW mode to produce the drive beams have been proposed [7]. To extend our study to these applications, we defined and investigated dimensionless parameters in this work. The definition of dimensionless parameters is introduced in the subsequent section.

2. Definition of the parameters

The LINAC must store more electromagnetic energy than total energy gain of the bunches in a pulse so that sufficient voltage is available in the cavity to accelerate the last bunch in the beam. To characterize the required relative stored energy in the cavity, a dimensionless parameter named capacity factor is defined as

$$\eta = \frac{U_c}{U_b}, \tag{1}$$

where U_b is the total energy gain of the bunches in a pulse, U_c is the required maximum electromagnetic energy stored in the cavity. η gives the required quantity of SRF structures for a normal RF system, considering that the stored energy in each SRF cavity is limited. A considerable amount of stored energy increases the losses on the superconducting wall and power consumption on cryogenics. Consequently, η is a crucial parameter in the total cost. The minimization of η is hence the main objective in this work.

The second dimensionless parameter is defined as

$$\kappa = \frac{\lambda q_b}{V_a}, \tag{2}$$

where λ is the loss factor of the full LINACs, q_b is the total beam charge in one pulse, and V_a is the designed acceleration voltage (2.4 GV for the CLIC SC-DB LINACs). κ is called the loading factor, which quantifies the relative beam loading. The relationship between the parameters η and κ is described as follows:

$$\eta = \frac{U_c}{U_b} = \frac{|V_{max}|^2/(2\lambda)}{V_a q_b} = \frac{|V_{max}|^2/V_a^2}{2\lambda q_b/V_a} = \frac{\left|\widetilde{V}_{max}\right|^2}{2\kappa} \tag{3}$$

where V_{max} is the maximum voltage in the cavity and $\widetilde{V}_{max}$ is normalized V_{max} scaled to the acceleration voltage.

The parameters of CLIC SC-DB LINACs for the 3 TeV stage are listed in Table 1.

Table 1
Parameters of CLIC SC-DB LINACs.

	Description	Value
U_b	Total energy gain of the bunches in one pulse	1.4 MJ
q_b	Total charge of one beam pulse	589 μC
V_a	Required accelerating voltage	2.4 GeV
N	Number of bunches in one pulse	70128
ω	Angular frequency of cavity	$2\pi * 500$ MHz
t_s	Bunch separation	2 ns
T_f	Time of energy-storing period	19.86 ms

3. Beam-loading effect

The beam-loading effect takes place when the beam induces an electromagnetic field when it passes through a cavity, and this induced field is added to the existing field in the cavity [27–32]. When the beam is at the accelerating phase, the beam-induced field cancels the existing field. This effect decreases the field amplitude in the cavity. The loss of stored electromagnetic energy in the cavity is then transferred to the spread of beam energy.

In regular accelerating structures, the energy consumption due to the beam-loading effect is typically replenished by external power sources [27–29]. The peak power from the sources is, however, far smaller than the peak power consumed by the beam in the energy-storing and energy-releasing scheme, as shown in Fig. 2. In this study, the power supply from external sources and power dissipation on the surfaces of superconducting wall are neglected. In this case, the beam-loading effect illustrated in a complex plane [30,31] as shown in Fig. 3 can be expressed by

$$\widetilde{V}_{n+1} = \frac{\left(V_n - \lambda\frac{q_b}{N}\right)e^{j\theta}}{V_a} = \left(\widetilde{V}_n - \frac{\kappa}{N}\right)e^{j\theta}, \tag{4}$$

where $\widetilde{V}_n$ is the normalized accelerating voltage seen by the nth bunch, and θ is the phase shift between the two bunches caused by the

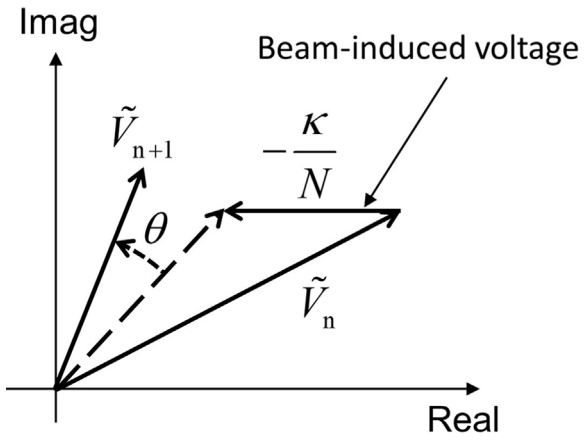

Fig. 3. Beam-loading effect in the complex plane.

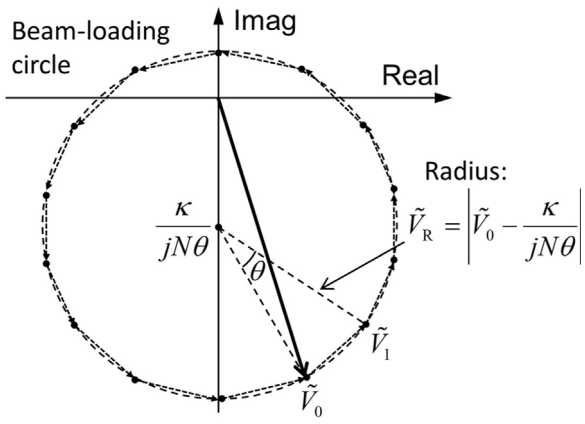

Fig. 4. Beam-loading effect on multiple bunches with fixed phase shift.

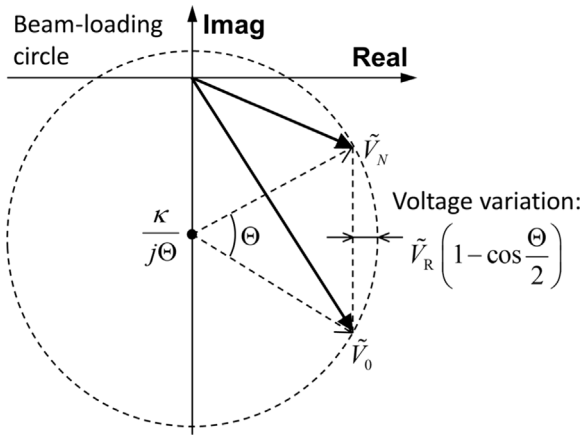

Fig. 5. Normalized accelerating voltage profile using the fixed phase shift scheme.

difference between the frequency of the cavities and the frequency of the beam bunches.

If $\theta = 0$, then Eq. (4) turns into

$$\widetilde{V}_n = \widetilde{V}_0 - \frac{\kappa n}{N}, \tag{5}$$

where $\widetilde{V}_0$ is the normalized initial voltage. The normalized average accelerating voltage must be 1. The accelerating voltage variance is hence

$$\left|\widetilde{V}_0 - \widetilde{V}_N\right| = \kappa, \tag{6}$$

which should be less than 1% given by the acceptable beam energy variation due to the high luminosity requirement [33,34]. According to Eq. (3), the capacity factor η can be derived as

$$\eta = \frac{\left|\widetilde{V}_0\right|^2}{2\kappa} \geq \frac{\left|1+\frac{\kappa}{2}\right|^2}{2\kappa}, \tag{7}$$

which is larger than 50.5 in this scheme.

When θ is a small fixed value, Eq. (4) can be approximately transformed to

$$\widetilde{V}_n = \frac{\kappa}{jN\theta} + \left(\widetilde{V}_0 - \frac{\kappa}{jN\theta}\right) e^{jn\theta}. \tag{8}$$

The trace of $\widetilde{V}_n$ shown in the complex plane is a circle with its center point at $\kappa/(jN\theta)$, as shown in Fig. 4. This circle is called beam-loading circle. Therefore, the normalized accelerating voltage Real($\widetilde{V}_n$) seen by each bunch is a cosine function of n, of which the amplitude and phase are determined by the initial voltage $\widetilde{V}_0$ and the period is determined by the phase shift θ.

In the application of this scheme in the CW CLIC SC-DB LINACs, the range near the peak of the cosine function is selected to obtain a flat voltage profile, as presented in Fig. 5, where $\Theta = N\theta$ is the total phase shift in a full beam pulse, and the amplitude of the cosine function is

$$\widetilde{V}_R = \left|\widetilde{V}_0 - \frac{\kappa}{j\Theta}\right|. \tag{9}$$

The average accelerating voltage and the voltage variation can be expressed as :

$$\overline{\text{Real}\left(\widetilde{V}_n\right)} = \frac{\int_{-\frac{\Theta}{2}}^{\frac{\Theta}{2}} \widetilde{V}_R \cos(\phi)\, d\phi}{\Theta} = \widetilde{V}_R \frac{2\sin\frac{\Theta}{2}}{\Theta} = 1, \tag{10}$$

$$\text{Max}\left(\text{Real}\left(\widetilde{V}_n\right)\right) - \text{Min}\left(\text{Real}\left(\widetilde{V}_n\right)\right) = \widetilde{V}_R\left(1-\cos\frac{\Theta}{2}\right). \tag{11}$$

Limited by the acceptable 1% voltage variation, the total phase shift Θ should be less than 16.2° according to Eq. (11). The capacity factor is then derived as

$$\eta = \frac{\left|\widetilde{V}_0\right|^2}{2\kappa} = \frac{\left|\widetilde{V}_R e^{-j\frac{\Theta}{2}} + \frac{\kappa}{j\Theta}\right|^2}{2\kappa} \geq \frac{\widetilde{V}_R}{\Theta}\left(1+\sin\frac{\Theta}{2}\right) = \frac{1+\sin\frac{\Theta}{2}}{2\sin\frac{\Theta}{2}}, \tag{12}$$

which is approximately 4.05 in the fixed phase shift scheme This capacity factor is much lower than that of Eq. (7) but still high. Therefore, new solutions must be explored to compensate this beam-loading effect with a lower capacity factor.

4. Beam-loading compensation schemes

4.1. Tuning structure scheme

The proposed scheme in this subsection utilizes time-varying phase shifts to ensure that all bunches have the same accelerating voltage. θ in Eq. (4) is hence the function of n The real part of $\widetilde{V}_n$ retains a value of 1 and the imaginary part of $\widetilde{V}_n$, changes with n in this case, as shown in Fig. 6. The differential equation of $\widetilde{V}_n$ can be expressed as

$$\frac{d\widetilde{V}_n}{dn} = -\frac{\kappa}{N} + j\theta_n\widetilde{V}_n = -\left(\frac{\kappa}{N} + \theta_n I_n\right) + j\theta_n = j\frac{dI_n}{dn}, \tag{13}$$

where θ_n is the phase shift between the nth and (n+1)th bunches, and I_n is the imaginary part of $\widetilde{V}_n$. Solving the real and imaginary part of this equation, the expressions of θ_n and I_n with n can be derived as

$$\theta_n = -\frac{\kappa}{N I_n}, \tag{14}$$

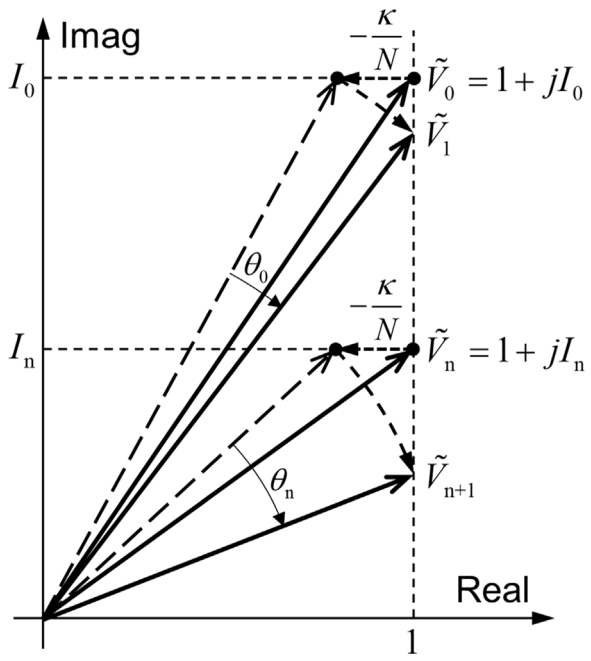

Fig. 6. Trace of $\tilde{V}_n$ in the complex plane for the tuning structure scheme.

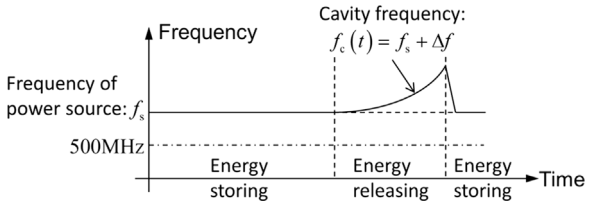

Fig. 7. Resonant frequency of cavities in a full cycle.

$$I_n = \sqrt{I_0^2 - \frac{2\kappa n}{N}}. \tag{15}$$

Eq. (15) shows that I_n drops as n increases, indicating that the amplitude of the field decreases after the bunches are accelerated. The absolute value of θ_n increases when I_n decreases according to Eq. (14). Given that the bunch separation t_s is fixed, the varying of phase $\theta_n = \omega t_s - 2k\pi$ can be done only by changing the angular frequency of cavity ω, where k is the number of RF power period between bunches and keeps a value of 1 in this work. The resonant frequency of the cavity remains the same as the frequency of the external sources during power storing and is changed by a fast tuner at beam time to fit the phase change provided by Eqs. (14) and (15), as shown in Fig. 7. This tuning frequency as a function of time, $\Delta f_n = \theta_n/(2\pi t_s)$, is called tuning function. The imaginary part of normalized accelerating voltage I_n should be a purely real number so that I_0^2 must be larger than 2κ derived from Eq. (15). Thus, η can be calculated from Eq. (3) as

$$\eta = \frac{\left|\tilde{V}_0\right|^2}{2\kappa} = \frac{1 + I_0^2}{2\kappa} \geq 1 + \frac{1}{2\kappa}, \tag{16}$$

which is achieved to be near 1 when the loading factor κ has a large value.

However, the tuning range and tuning speed are restricted in actual operations, which limits the capacity factor η. Given that $|\Delta f_n|$ is a monotonically increasing function of n as presented in Fig. 7, the maximum tuning range Δf_R and the maximum tuning speed v_f are defined as

$$\Delta f_R = \mathrm{Max}\left(|\Delta f_n|\right) - \mathrm{Min}\left(|\Delta f_n|\right)$$

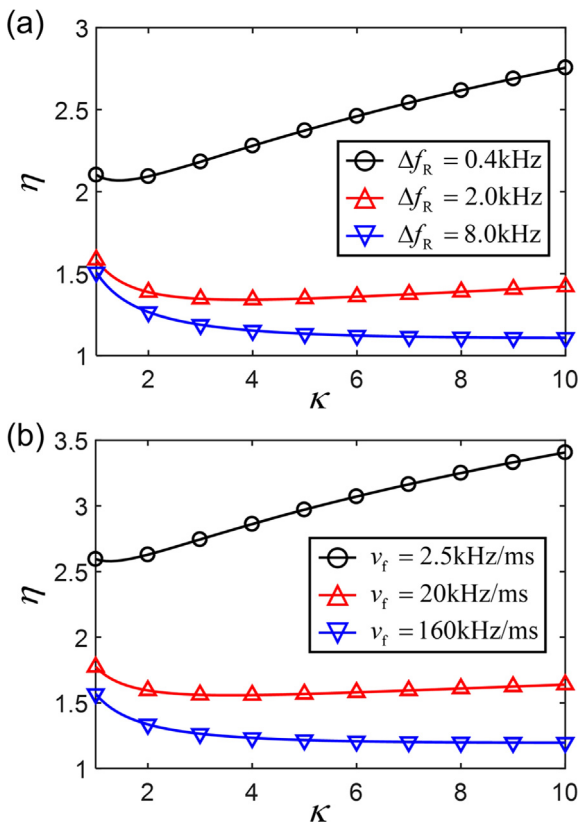

Fig. 8. The capacity factor η versus the loading factor κ, limited by the (a) tuning range and (b) tuning speed.

$$= \frac{\kappa}{2\pi t_s N}\left(\frac{1}{\sqrt{2\kappa(\eta-1)-1}} - \frac{1}{\sqrt{2\kappa\eta - 1}}\right), \tag{17}$$

$$v_f = \mathrm{Max}\left(\frac{d\left|\Delta f_n\right|}{t_s dn}\right) = \frac{\kappa^2}{2\pi t_s^2 N^2\left(\sqrt{2\kappa(\eta-1)-1}\right)^3}, \tag{18}$$

respectively. Referring to the maximum tuning range and speed from SRF cavity designed for International Linear Collider (ILC) [35] and scaling the cavity frequency to 500 MHz, the maximum speed of the tuner can reach 2.5 kHz/ms. Based on the current technologies and the parameters of the CLIC 3-TeV stage listed in Table 1, the optimum η is 2.58 in this scheme as shown in Fig. 8.

The tuning sensitivity of 500 MHz cavity is about 160 Hz/μm. If the piezo tuner can reach a speed of 1 m/s and the stroke is 50 μm, a larger tuning range of 8 kHz and a faster tuning speed of 160 kHz/ms can be achieved. The optimum η is hence approximately 1.20. However, the technologies of the tuner working at this tuning speed are not yet developed. Considering the complex response of the frequency tuning in the full RF system, the capacity factor η will be worse than the rough estimations calculated above. Detailed analysis on this tuning scheme is worthy to be investigated after a critical advance on the tuning technologies of the SC cavity in the future.

4.2. Mixed-structure scheme

Another scheme is proposed in this subsection to correct the voltage variation by utilizing additional correction structures with different phase shifts, as shown in Fig. 9. The accelerating structures provides an unflattened voltage profile and has a large total phase shift Θ_0 to decrease the fundamental capacity factor η_0 based on Eq. (12). The difference between the unflattened voltage profile and the ideal

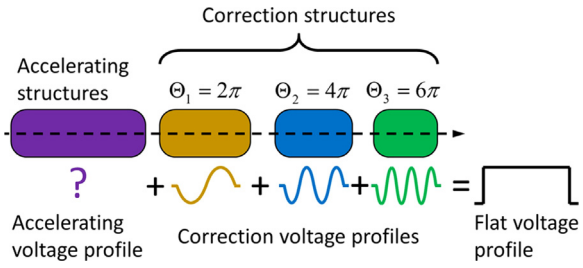

Fig. 9. Schematic layout of the mixed-structure scheme.

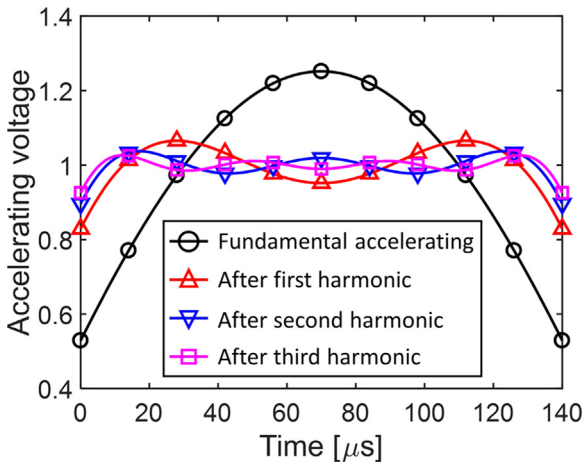

Fig. 10. Voltage profile of the accelerating and correction structures.

flat voltage profile can be decomposed by the Fourier series. Similar ideas can also be found in Refs. [36–38]. Each Fourier series refers to a correction structure, which provides the harmonic cosine-function voltage profile to compensation the voltage variation, as presented in Fig. 10.

The total phase shift of the fundamental structure, Θ_0, is a crucial parameter because it determines the voltage amplitude of the mth correction structure, H_m, provided by each correction structure, which is expressed as

$$\begin{aligned} H_m &= -2\int_{-1/2}^{1/2} H_0(t)\cos(\Theta_m t)\,dt \\ &= -2\int_{-1/2}^{1/2} \frac{\Theta_0}{2\sin\frac{\Theta_0}{2}}\cos(\Theta_0 t)\cos(\Theta_m t)\,dt \\ &= \frac{(-1)^m 2\Theta_0^2}{\Theta_m^2-\Theta_0^2}, \end{aligned} \tag{19}$$

where $H_0(t)$ is the voltage profile of the accelerating structure, $\Theta_m = 2m\pi$ is the total phase shift over the full bunch train of the mth correction structure. The maximum voltage amplitude of a correction structure is not the initial voltage because the structure may gain energy from the beam. The maximum voltage amplitude point of a correction structure is located at the bottom point of the beam-loading circle shown in Fig. 5, where $\left|\tilde{V}_R\right| = |H_m|$. The capacity factor of the mth correction structure is hence written as

$$\eta_m = \frac{\left(|H_m| + \frac{\kappa_m}{\Theta_m}\right)^2}{2\kappa_m} \geq \frac{2|H_m|}{\Theta_m} = \frac{4\Theta_0^2}{\Theta_m\left(\Theta_m^2-\Theta_0^2\right)} \tag{20}$$

based on Eq. (3), where κ_m is the loading factor of the mth correction structure. η_m reaches its minimum when $\kappa_m = |H_m|\Theta_m$. The capacity factor of the accelerating structure η_0 is calculated by Eq. (12). Therefore, the total capacity factor for all the structures, $\eta = \sum\eta_m$, is a function

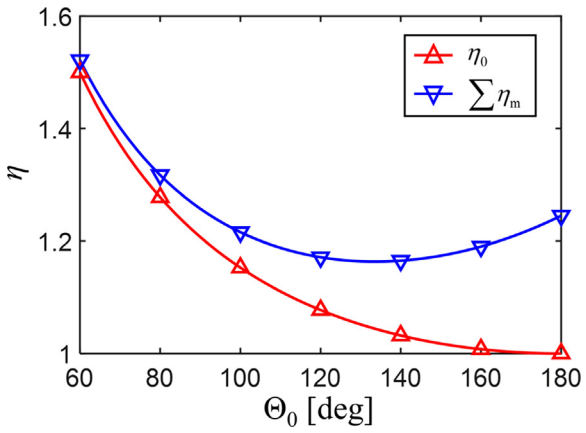

Fig. 11. Total capacity factor versus Θ_0 in the mixed-structure scheme.

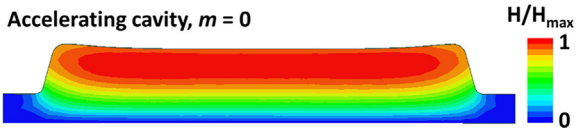

Fig. 12. Geometries and magnetic field plots of the accelerating cavity for the CLIC 3 TeV stage.

of Θ_0 and can be numerically solved, as presented in Fig. 11. The optimum η for this mixed-structure scheme is approximately 1.16 when Θ_0=134°. The total number of SRF structures can be reduced compared to the scheme of all structures with the same fixed-phase shift although the correction structures are added.

5. Cost estimation

The mixed-structure scheme is preferable for the design of the CLIC SC-DB LINACs due to the lower capacity factor, as discussed in Section 4. The cost of this scheme is estimated and compared with that of the baseline NC-DB LINACs in this section.

The CLIC baseline design utilizes only one DB LINAC to feed both electron and positron sites in the 380 GeV and 1.5 TeV stages. Therefore, the total charge of one beam pulse q_b in 380 GeV stage is 1/4 of that in the final 3 TeV stage. The normalized shunt impedance per cavity R/Q is a crucial parameter depending on q_b, which is expressed as

$$\frac{R}{Q} = \frac{2U_M}{\omega q_b^2}\frac{\kappa_m}{\eta_m} = \frac{2U_M}{\omega q_b^2}\times\begin{cases}\dfrac{\Theta_0^2}{1+\sin\frac{\Theta_0}{2}}, m=0\\ 2m^2\pi^2, m\geq 1\end{cases}, \tag{21}$$

where U_M is the maximum stored energy in one SRF cavity. To achieve the minimum η in the mixed-structure scheme, the capacity factor η_m and the loading factor κ_m of each structure are assigned values. Consequently, the optimum cavity geometry in the earlier stages is not the optimum design for the final stage due to the different q_b, which causes difficulties in reusing SRF cavities of earlier stages in future upgrades and possibly increases the cost. A feasible strategy is to reuse the fundamental accelerating structure cavities of the earlier stages as the correction structure cavities for the later stages and to reuse the correction structure cavities with smaller harmonic number m as the ones with higher m in the upgrades. This strategy could achieve a good match of both quantities and the shunt impedance of cavities among stages. In this case, η for the 380 GeV and the final 3 TeV stages are 1.27 and 1.18, respectively.

A preliminary design for the accelerating cavity for the 3 TeV stage were simulated by HFSS code [39] to roughly estimate parameters

Table 2
RF parameters of the accelerating cavity for 3 TeV stage.

Parameters	Accelerating cavity
Frequency	500 MHz
Effective length	1.40 m
Beam pipe radius	90 mm
Maximum stored energy in one SRF cavity U_M	1210 J
R/Q	5.9 Ω/m
Geometrical factor	413 Ω
Q_0	5×10^{10}
Q_{ext}	2.5×10^7
Dynamic heating at 2 K	35.6 W
Maximum coupler power	70 kW
Maximum accelerating gradient	5.6 MV/m
Average operated gradient	3.7 MV/m
Maximum surface E-field	47 MV/m
Maximum surface B-field	120 mT

Table 3
Estimations of the SC LINACs and the NC LINACs for the CLIC drive beam.

Parameters	SC LINACs		NC LINACs	
	380 GeV	3 TeV	380 GeV	3 TeV
Number of cavities	360	2800	446	1080
Number of klystrons	45	435	446	1080
Klystron power	420 kW	420 kW	22 MW	22 MW
Length of one LINAC [km]	0.67	2.6	2.0	2.5
Total AC power [MW]	52	382	49	305
Cost [BCHF]	0.58	4.08	1.2	2.7

and related cost, as shown in Fig. 12. Nitrogen-doped niobium is used as the superconductor material. The material processing of PIP-II HB-650 cavities is took as the references [22]. The tests on PIP-II HB-650 cavities at Fermilab have shown that an excessively high quality factor Q_0 of 5×10^{10} at 2 K was achieved at the gradient of 30 MV/m with the peak B-field of 125 mT [23]. Cavities of SC-DB LINAC have a lower working frequency and a lower peak surface B-field as listed in Table 2. Therefore, Q_0 of 5×10^{10} seems promising for the CLIC SC-DB cavities with a maximum surface B-field of 120 mT. The harmonic cavities can be designed in terms of the superconductor material, Q_{ext}, and beam pipe diameter in the similar manner. The design and performances of the cavities will be updated and improved in pace with the development of the groundbreaking technologies on the SRF.

A rough estimation of the CLIC SC-DB LINAC is summarized in Table 3 and compared with that of the baseline NC design. For the 3 TeV stage, the SC-DB LINACs have similar length as that of baseline NC LINACs. AC power consumption from klystrons was calculated based on the 70% efficiency for both design [2]. With the 11% efficiency loss of modulators, the NC LINACs demand more electricity for the RF power generation. However, the cryogenic power is significant for SC LINACs to make the total power consumption larger. The cost estimation of CLIC SC-DB LINACs takes the HP-SPL [24] and LHC [26] as the references. Compared with the costs of the baseline NC LINACs, the design studied in this work shows a potentially lower entry cost but more expensive at later stages than the baseline design.

The cost of SC-DB LINACs is dominated by the cost of SRF cavities (40%) and cryogenics (35%). The cavity geometries have a lower surface B-field and a larger geometrical factor. A higher Q_0 might be achieved to reduce the cryogenic power. The 500 MHz cavities are capable of working at 4.5 K, which may significantly reduce the cryogenic power. The number of cavities and related cost could be reduced if a higher cavity stored energy U_M is achieved in the future investigation. U_M is limited by the surface magnetic field, which can be improved by the SRF material processing. If U_M could reach 1800 J, the cost of SC-DB LINACs for 3 TeV stage can be reduced to 3.1 BCHF, which is approximately at the same level of the baseline NC design. In this case, the benefit of the lower entry cost will make the design of SC-DB LINACs more attractive.

6. Conclusion

The superconducting LINAC design, which utilizes energy-storing and energy-releasing scheme for the CLIC drive beam, is investigated in this work. This scheme stores the RF energy in SRF structures operating in CW mode and releases the energy when the beam comes. Fewer power sources and structures are required in the early stages using this scheme. Investigation on this scheme is worthy for its potential to reduce the entry cost.

The beam-loading effect causes the decline in the accelerating voltage during the energy-releasing period. Therefore, cavities must store RF energy more than that absorbed by the beam such that the last bunch in the beam pulse still has sufficient voltage. A dimensionless factor η is defined to determine that the RF energy must be stored in the cavity with regard to the absorbed RF energy in the beam. This capacity factor η is an extremely crucial parameter because it determines the number of the SRF structures and the cryogenics power, which are related to the total cost. The value of η will be larger than 50.5 to achieve the 1% voltage variation if the beam-loading effect is not compensated. Two proof-of-concept schemes to compensate the beam-loading effect are proposed in this work.

One is the tuning structure scheme. The resonant frequency of the accelerating cavity is changed to obtain the appropriate phase for all bunches such that all bunches can have the same accelerating field. The real-time frequency change is implemented by the fast tuner on the cavity wall. This scheme could achieve a minimum η of 2.58 for the CLIC 3-TeV stage based on the current technologies. The main limitation of reducing η is the tuning range and speed of the fast tuner.

The other scheme is the mixed-structure scheme. The structure shifts from a fixed frequency to the beam frequency and provides an accelerating voltage profile in a cosine function to all the bunches. Structures with different frequency shifts provide cosine functions at different periods, and this process forms a flat voltage profile by using the Fourier series. This scheme has an optimum η of approximately 1.16.

The mixed-structure scheme is selected as the nominal design of CLIC SC-DB LINACs now. The preliminary parameters and costs of the CLIC SC-DB LINACs for the initial 380 GeV stage and the final 3 TeV stage have been roughly estimated, which demonstrates that the SC LINAC design may reduce the entry cost. Detailed technical issues will be investigated in the future.

CRediT authorship contribution statement

Jiayang Liu: Conceptualization, Methodology, Investigation, Writing - review & editing. **Alexej Grudiev:** Conceptualization, Writing - review & editing, Supervision. **Hao Zha:** Conceptualization, Methodology, Investigation, Writing - original draft, Supervision. **Jiaru Shi:** Supervision. **Huaibi Chen:** Supervision.

Declaration of competing interest

The authors declare that they have no known competing financial interests or personal relationships that could have appeared to influence the work reported in this paper.

Acknowledgments

The authors would like to thank Philippe Lebrun, Walter Wuensch, Daniel Schulte, Igor Syratchev, and Andrea Latina for their helpful discussions.

References

[1] R. Tomás, Overview of the compact linear collider, Phys. Rev. Special Top. Accel. Beams 13 (2010) 014801.

[2] CLIC and CLICdp collaborations, A Multi-TeV Linear Collider Based on CLIC Technology, CLIC Conceptual Design Report, CERN, Geneva, Switzerland, 2012, CERN-2012-007.

[3] M. Voin, L. Schächter, Linear analysis of active-medium two-beam accelerator, Phys. Rev. Special Top. Accel. Beams 18 (2015) 071302.

[4] T.M. Jain, N. Antonsen Jr, J.P. Palastro, Positron acceleration by plasma wakefields driven by a hollow electron beam, Phys. Rev. Lett. 115 (2015) 195001.

[5] M. Litos, E. Adli, W. An, et al., High-efficiency acceleration of an electron beam in a plasma wakefield accelerator, Nature 515 (2014) 92–95.

[6] W. Gai, Two beam wakefield acceleration at argonne wakefield accelerator facility, in: Proc. 7th International Particle Accelerator Conference (IPAC'16), Busan, Korea, 2016, pp. 4258-4260.

[7] A. Zholents, W. Gai, R. Lindberg, et al., A collinear wakefield accelerator for a high repetition rate multi beamline soft X-ray FEL facility, in: Proc. 36th International Free Electron Laser Conference (FEL2014), Basel, Switzerland, 2014, pp. 993-998.

[8] C. Jing, S. Antipov, P. Schoessow, et al., Argonne Flexible Linear Collider, in: Proc. 4th International Particle Accelerator Conference (IPAC'13), Shanghai, China, 2013, pp. 1322-1324.

[9] W. Gai, J. Power, C. Jing, Short-pulse dielectric two-beam acceleration, J. Plasma Phys. 78 (2012) 339.

[10] S.Y. Kazakov, S. Kuzikov, Y. Jiang, J. Hirshfield, High-gradient two-beam accelerator structure, Phys. Rev. Special Top. Accel. Beams 13 (2010) 071303.

[11] Y.S. Derbenev, Y. Lau, R. Gilgenbach, Proposal for a novel two-beam accelerator, Phys. Rev. Lett. 72 (1994) 3025.

[12] A.M. Sessler, D.H. Whittum, J.S. Wurtele, et al., Standing-wave free-electron laser two-beam accelerator, Nucl. Instrum. Methods Phys. Res. A 306 (1991) 592–605.

[13] A.M. Sessler, S.Y. Simon, Relativistic klystron two-beam accelerator, Phys. Rev. Lett. 58 (1987) 2439.

[14] D. Hopkins, A.M. Sessler, J. Wurtele, The two-beam accelerator, Nucl. Instrum. Methods Phys. Res. A 228 (1984) 15–19.

[15] W. Schnell, A two-stage rf linear collider using a superconducting drive linac, 1986, CERN-LEP-RF-86-06.

[16] L. Thorndahl, Drive Beam Generation for CLIC Based on 200 MHz SC Structures, 1998, CLIC-Note-352.

[17] H.H. Braun, R. Corsini, T.E. D'Amico, et al., The CLIC RF power source: a novel scheme of two-beam acceleration for electron-positron linear colliders, CERN-99-06, Geneva, Switzerland, 1999.

[18] R. Corsini, A. Ferrari, L. Rinolfi, et al., Experimental results on electron beam combination and bunch frequency multiplication, Phys. Rev. Special Top. Accel. Beams 7 (2004) 040101.

[19] CLIC and CLICdp collaborations, Updated Baseline for a Staged Compact Linear Collider, CERN, Geneva, Switzerland, 2016, CERN-2016-004.

[20] A. Gerbershagen, D. Schulte, P. Burrows, Compact linear collider drive beam phase stabilization simulations, Phys. Rev. Special Top. Accel. Beams 18 (2015) 041003.

[21] A. Aksoy, D. Schulte, Ö. Yavaş, Beam dynamics simulation for the compact linear collider drive-beam accelerator, Phys. Rev. Special Top. Accel. Beams 14 (2011) 084402.

[22] The PIP-II Collaboration, The PIP-II Reference Design Report, Fermi National Accelerator Laboratory, 2015.

[23] S. Mishra, Fermilab PIP-II Status and Strategy, in: Proc. the 57th ICFA Advanced Beam Dynamics Workshop on High-Intensity, High Brightness and High Power Hadron Beams (HB2016), Malmö, Sweden, 2016.

[24] F. Gerigk, Cost Estimate for the High Power SPL (HP-SPL), CERN, Geneva, Switzerland, 2012, sLHC-Project-Note-0037.

[25] LHC Study Group, The Large Hadron Collider: Conceptual Design, CERN, Geneva, Switzerland, 1995, CERN-AC-95-05-LHC..

[26] P. Lebrun, Private communication, 2016.

[27] O. Kononenko, A. Grudiev, Transient beam-loading model and compensation in compact linear collider main linac, Phys. Rev. Special Top. Accel. Beams 14 (2011) 111001.

[28] A. Lunin, V. Yakovlev, A. Grudiev, Analytical solutions for transient and steady state beam loading in arbitrary traveling wave accelerating structures, Phys. Rev. Special Top. Accel. Beams 14 (2011) 052001.

[29] N. Towne, J. Rose, Beam loading compensation of traveling wave linacs through the time dependence of the rf drive, Phys. Rev. Special Top. Accel. Beams 14 (2011) 090402.

[30] P.B. Wilson, J.E. Griffin, High energy electron linacs; application to storage ring RF systems and linear colliders, AIP Conf. Proc. 87 (1982) 450–582.

[31] M.G. Minty, R.H. Siemann, Heavy beam loading in storage ring radio frequency systems, Nucl. Instrum. Methods Phys. Res. A 376 (1996) 301–318.

[32] M.D. Kelisani, S. Doebert, M. Aslaninejad, An analytical approach for beam loading compensation and excitation of maximum cavity field gradient in a coupled cavity-waveguide system, Nucl. Instrum. Methods Phys. Res. A 828 (2016) 132–144.

[33] D. Schulte, A. Andersson, S. Bettoni, et al., Status of the CLIC phase and amplitude stabilisation concept, in: Proc. 25th Linear Accelerator Conference (LINAC2010), Tsukuba, Japan, 2010, pp. 103-105.

[34] D. Schulte, Private communication, 2016.

[35] N. Phinney, N. Toge, N. Walker, International Linear Collider Reference Design Report: ILC Global Design Effort and World Wide Study, 2007, ILC-REPORT-2007-001.

[36] S. Kashiwagi, H. Hayano, K. Kubo, et al., Beam test of multi-bunch energy compensation system in the accelerator test facility at KEK, Japan. J. Appl. Phys. 43 (2004) 5617–5622.

[37] L.R. Carver, R.M. Jones, Y. Jiang, J.L. Hirshfield, Longitudinal stability in multiharmonic standing wave linacs, Phys. Rev. Accel. Beams 19 (2016) 094001.

[38] Y. Huang, H. Wang, R.A. Rimmer, et al., Multiple harmonic frequencies resonant cavity design and half-scale prototype measurements for a fast kicker, Phys. Rev. Accel. Beams 19 (2016) 122001.

[39] Ansys HFSS, https://www.ansys.com/products/electronics/ansys-hfss.